Published in final edited form as:
Science. 2020 November 27; 370(6520): 1105–1110. doi:10.1126/science.abc7782.

Elongational Stalling Activates Mitoribosome-associated Quality Control

Nirupa Desai[#1], **Hanting Yang**[#1], **Viswanathan Chandrasekaran**[#1], **Razina Kazi**[1], **Michal Minczuk**[2], **V. Ramakrishnan**[1,*]

[1]MRC Laboratory of Molecular Biology, Cambridge CB2 0QH, UK

[2]MRC Mitochondrial Biology Unit, University of Cambridge, Hills Road, Cambridge CB2 0XY, UK

[#] These authors contributed equally to this work.

Abstract

The human mitochondrial ribosome (mitoribosome) and associated proteins regulate the synthesis of 13 essential subunits of the oxidative phosphorylation complexes. We report the discovery of a mitoribosome-associated quality control pathway that responds to interruptions during elongation, and present structures at 3.1 and 3.3 Å resolution of mitoribosomal large subunits trapped during ribosome rescue. Release factor homolog C12orf65 (mtRF-R) and RNA-binding protein C6orf203 (MTRES1) eject the nascent chain and peptidyl tRNA, respectively, from stalled ribosomes. Recruitment of mitoribosome biogenesis factors to these quality control intermediates suggest additional roles for these factors during mitoribosome rescue. We also report related cryo-EM structures (3.7 – 4.4 Å) of elongating mitoribosomes bound to tRNAs, nascent polypeptides, the GTPase elongation factors mtEF-Tu and mtEF-G1, and the Oxa1L translocase.

Mitochondria are double-membrane organelles with important roles in metabolism and ATP generation. They have retained many features of their a-proteobacterial ancestry, including their own genome and ribosomes (mitoribosomes). We and others have determined structures of mitoribosomes from various eukaryotes (1–4). Human mitoribosomes comprise a 39S large subunit (LSU) [52 proteins, a 16S ribosomal RNA (rRNA) and mt-tRNA^{Val}] and a 28S small subunit (SSU) [30 proteins and a 12S rRNA] and synthesize 13 inner mitochondrial membrane proteins encoded by mitochondrial DNA. These proteins are co-translationally inserted into the mitochondrial inner membrane by the Oxa1L translocase, where they are assembled with nuclear-encoded components into oxidative phosphorylation complexes.

Little is known about mechanisms of co-translational ribosome-associated quality control (RQC) in mitochondria, and if they exist, whether they operate any differently from those

[*]Corresponding author. ramak@mrc-lmb.cam.ac.uk.

Author Contributions: N.D and H.Y performed cell biology, biochemistry, sample preparation and cryo-EM data collection; R.K purified recombinant proteins and V.C. performed the hydrolysis experiments. M.M provided key research material; V.C and N.D processed data, determined and interpreted structures, V.C built and refined models; N.D. and V.C. wrote the manuscript with input from all authors; V.R oversaw the project and edited the manuscript.

Competing interests: The authors declare no competing interests.

Europe PMC Funders Author Manuscripts

present in bacteria and the eukaryotic cytosol (5). Stalling can occur at any step of the translation cycle due to defective mRNAs, including absent in-frame stop codons, truncations or inappropriate polyadenylation within the protein coding region (6), and tRNA mutations or insufficiency (7). In these and other cases, RQC is critical to maintain cellular homeostasis by rescuing stalled ribosomes, preventing protein misfolding and other aberrant translation phenotypes (8, 9). Mitochondria however lack counterparts to bacterial rescue mechanisms such as *trans*-translation, stringent control, and ArfA (10). ICT1, the presumed mitochondrial ortholog of another bacterial rescue factor ArfB, was instead identified as an integral component of the LSU (1, 3, 11). *In silico* studies have proposed that other putative mitochondrial release factors may exist, but without biochemical evidence (10).

We reasoned that any attempt to induce translational stalling might trap mitoribosomes at various stages of the translation cycle in the act of nascent chain insertion into the inner mitochondrial membrane, and generate intermediates suitable for structural analyses by cryo-EM. We therefore purified mitoribosomes from a genetically engineered human cell line that lacks the 2'-5' phosphodiesterase exonuclease 12 (PDE12). PDE12 facilitates the maturation of mt-tRNA, mt-tRNA^{Lys} in particular, by deadenylating spurious poly(A) tails from mt-tRNAs and restoring the 5'-CCA-3'. A PDE12 knockout can therefore lead to aberrant polyadenylation of the 3' ends of mt-tRNAs and consequently, ribosome stalling (12). During purification we included GMPPCP, a non-hydrolysable GTP analog, to prevent dissociation of GTPases, mtEF-G1 and mtEF-Tu, from mitoribosomes, and n-Dodecyl β-D-maltoside (β-DDM) to solubilize mitoribosomes anchored to the mitochondrial inner membrane via the Oxa1L translocase (13) (Figure S1). Exhaustive classification of over 3 million mitoribosomes imaged using cryo-EM yielded several structures at resolutions of 3.1 – 4.4 Å (Table S1, Figure S2, S3, S4).

As expected, we observed a substantial proportion of stalled mitoribosomes. We also observed two classes of LSUs with attached tRNA(s) and nascent polypeptide (Figure 1). The presence of a nascent chain attached to a tRNA confirms that these classes represent LSUs of ribosomes that have been split *before* termination and nascent chain hydrolysis have occurred. Therefore, they represent intermediates in a hitherto unreported mitoribosome-associated quality control (mtRQC) pathway.

The first LSU class was resolved to 3.1 Å resolution and harbors both P- and E-site tRNAs (Figure 1A). The tRNAs are secured by bridging interactions with elements of vicinal proteins and other unassigned densities that span the inter-tRNA space (Figure S5A). The Esite tRNA is further stabilized by D-loop interactions with uL1m, similar to those seen in bacterial and mammalian structures (Figure 1A, inset) (14). We conclude that this class represents an early mitoribosome-associated quality control intermediate that has been split by an unknown mechanism upon stalling.

The second LSU class, determined to 3.3 Å resolution, represents a rescue intermediate prior to hydrolysis of the nascent chain. The resolution of this complex permitted unambiguous identification and modeling of two proteins. The complex contains a peptidyl-tRNA that has recruited a heterodimer of the release factor homolog C12orf65 (here renamed 'mtRF-R' for mitochondrial Release Factor in Rescue) and MTRES1, a double-stranded RNA (dsRNA)

binding protein (Figure 1B, C, S5B). There was excellent agreement between the protein sequences and most side chain densities (Figure 1C). mtRF-R occupies the A site of the LSU next to the peptidyl tRNA, whereas MTRES1 wraps around the anticodon stem-loop of the peptidyl tRNA (Figure 2A, Figure S6A). The two proteins interact via the C-terminal helix of mtRF-R and the S4-like domain of MTRES1. The observed binding of mtRF-R and MTRES1 is consistent with their co-immunoprecipitation from HEK293T cells (15).

mtRF-R structurally resembles the GGQ-containing catalytic domain of the bacterial release factors RF1 and RF2. Like RF1/2, mtRF-R inserts a conserved GGQ motif into the peptidyl transferase center (PTC) (Figure 1D). One major difference is that the C-terminal helix of mtRF-R has split into two a-helices (α_1 and α_2), whereas in bacterial release factors, the equivalent helix (α_7) is continuous (Figure 2A, B). The long α_2-helix of mtRF-R, which extends to contact MTRES1, is stabilized by the tip of helix 69 of 16S rRNA (Figure S6A, B). In addition to the α_2-helical contacts, conserved Arg99 of the GGQ domain hydrogen-bonds with C71 of the terminal 3'CCA, and Gln103 contacts position 1 of the tRNA (Figure S6C).

The modeled residues of MTRES1 (129-216) bind the anticodon stem-loop of the P-site tRNA as well as helix 69 rRNA and the C-terminus of the α_2-helix of mtRF-R (Figure S6, S7). MTRES1 was predicted to contain an S4-like double-stranded RNA binding domain (15). This region binds helix 69 and resembles the corresponding domain of the *E. coli* ribosomal protein uS4, despite having only 15% sequence identity (Figure 2C, D). Other regions outside the S4-like domain have diverged considerably to confer tRNA and mtRF-R binding ability. The conserved α_1 and α_2 helices of the S4-like domain make specific contacts with helix 69 of the 16S rRNA (Figure S6D). MTRES1 also interacts with a double-stranded region of the peptidyl tRNA (Figure S6E), where stabilizing contacts are made between positive residues of β_1 and β_4 against the backbone of positions 24, 36 and 37 of the tRNA. MTRES1 and mtRF-R interact with each other predominantly using the C-termini of their respective α_2 helices, via a salt bridge and a network of hydrogen bonds and hydrophobic interactions (Figure S6F).

Comparison of the two post-splitting classes reveals the order of events along the mtRQC pathway. We conclude that the first class is an early post-splitting state of the LSU that serves as the substrate for mtRF-R to bind the empty aminoacyl site in the PTC. Concomitant binding and repositioning of the peptidyl tRNA by MTRES1 (compare peptidyl tRNA positions in Figure 2A, B) would eject the E-site tRNA and allow the mtRF-R/MTRES1 heterodimer to hydrolyze the nascent chain and extract the tRNA. RQC pathways must target the small population of stalled ribosomes while sparing the majority of active ribosomes from futile rescue. This pathway is specific for stalled and split mitoribosomal LSUs because: (i) actively translating ribosomes rarely persist with an empty A site, (ii) the kinked α_1-α_2 arrangement of mtRF-R would sterically clash with an SSU if present, and (iii) mtRF-R is stabilized by packing against MTRES1, an ordered helix 69 of the 16S rRNA and the peptidyl tRNA, all of which are absent in empty LSUs.

In this LSU class undergoing rescue (Figure 1B), nascent chain hydrolysis has not occurred owing to unfavorable geometry between the attacking and leaving groups (Figure 1D) (16).

Although our map likely contains averaged density from many mitochondrial nascent peptides, it is also consistent with a lysyl residue in the PTC in a flipped position that we and others observed in mammalian cytosolic ribosomes stalled on poly(A) and with a poly-lysine nascent chain (16). The e nitrogen of the glutamine is methylated as seen in other release factors but is ~4.8 Å away from the carbonyl carbon of the lysyl residue, which is too far for a nucleophilic attack on the ester bond and could explain why the nascent chain has not yet been hydrolyzed. Our structure raises the question of whether mtRF-R can hydrolyze a suitable substrate *in vitro*. Among the putative mitochondrial release factors, only mtRF1a, the canonical mitochondrial termination factor and ICT1, a constitutive 39S protein have proven peptidyl-tRNA hydrolase activities, but previous *in vitro* experiments that failed to detect mtRF-R activity were performed without MTRES1 and used intact bacterial 70S ribosomes as substrate (11, 17, 18). We therefore reasoned, based on our structure, that mtRF-R too may hydrolyze bacterial ribosome-nascent chains (RNCs), provided (i) 70S-RNCs are first split into 50S-RNCs and (ii) MTRES1 is also present. This is indeed the case (Figure S8) showing that mtRF-R acts as a release factor on stalled LSU tRNA-nascent chains.

The importance of this rescue pathway is highlighted by the fact that mtRF-R is essential for mitochondrial protein synthesis (19, 20) and that mutations lead to human disease phenotypes (10), especially the triad of optic atrophy, peripheral neuropathy and spastic paraparesis. Autosomal recessive mutations result in mtRF-R truncations, the extent of which largely, but not exclusively, correlate with severity of disease phenotypes (17, 19, 20) (Figure S9). At the same time, MTRES1-knockout human cells exhibit reduced mitochondrial translation and oxidative phosphorylation deficiency (15).

The mtRF-R/MTRES1 mtRQC pathway is reminiscent of, but differs mechanistically from the eukaryotic cytosolic system of the yeast tRNA endonuclease Vms1 (ANKZF1 in human) and the ABCF-type ATPase Arb1 (21, 22). Both systems address the cellular need to release nascent chains from stalled ribosomal large subunits but operate via nascent chain hydrolysis and tRNA nucleolytic cleavage, respectively. Analogously to bacterial and mammalian RQC, the mitoribosomal mRNA and nascent chain must be extracted following hydrolysis and targeted for degradation.

Previous work identified a module of three factors, MALSU1 (mitochondrial assembly of ribosomal large subunit 1, C7orf30), L0R8F8, and mt-ACP (mitochondrial acyl carrier protein) that functions during mitoribosome biogenesis to bind immature LSUs and prevent premature subunit association (23). Intriguingly, we find the same MALSU1/L0R8F8/mt-ACP module on both the early post-splitting, and later rescue intermediates (Figure 1A, B), suggesting that the module is recruited to block subunit joining during tRNA and nascent chain removal from the split LSU. Other regulatory factors such as eIF6, ABCE1, and eIF3 prevent premature subunit joining during ribosome biogenesis, initiation and ribosome recycling after termination as well as after ribosome rescue (23–27). We propose that the MALSU1/L0R8F8/mt-ACP module functions during both biogenesis and rescue by preventing subunits of mitoribosomes from associating prematurely.

In addition to the two rescue pathway intermediates described above, our dataset also captured all of the main states during normal translational elongation by mitoribosomes except for one (Figure 3, 4). One intermediate (Figure 3A, S10A) has stalled with an empty A site and is likely rescued by mtRQC. Another observed class captures a state during decoding (Figure 3B, S10B) and contains a pre-accommodated mt-tRNA delivered to the A site of the mitoribosome by mtEF-Tu•GMPPCP. The mitochondrial ternary complex (Figure S10C, S11A-C) closely resembles the equivalent GMPPCP-bound complex on the bacterial ribosome. The decoding nucleotides A1561 and A1562 of helix 44 in the 12S rRNA (*E. coli* A1492 and A1493) both flip out to read the minor groove of the double-stranded helix formed between the +1, +2 and +3 A-site mRNA nucleotides and the anticodon of the A/T tRNA (Figure S10B, S11D). As in other ribosomes, correct decoding induces domain closure, a large scale movement of the body of the SSU that activates GTP hydrolysis and tRNA accommodation (28).

Domain closure is also observed in mitoribosomes with an accommodated cognate tRNA in the A site (A/A, P/P, E/E; Figure 3C) but not in ribosomes with an empty A site (Figure 3A). The poor local resolution in the former class precluded direct visualization of the ester bond between either tRNA and the nascent chain, but the absence of a P/E hybrid tRNA implies that peptidyl transfer has not yet occurred. Particles in which peptidyl transfer has already occurred are also present in the dataset, resulting in mitoribosomes in the rotated-1 state with A/A and P/E tRNAs (Figure 3D). mRNA, tRNA, rRNA and protein interactions observed in the mtEF-Tu-bound map (Figure 3B, S10B, S11D) are preserved in the decoding center of the mitoribosome bound to A, P and E tRNAs (Figure 3C).

In contrast, decoding centers of stalled mitoribosomes have rearranged significantly (Figure 3A; inset, S10A). In the absence of PDE12, these ribosomes have likely stalled with AAG or AAA codons in the A site (12). Consecutive AAA codons such as those in poly(A) tails have a particular propensity to base-stack in the decoding center even without stabilizing Watson-Crick base-pairing interactions with an A-site anticodon (16). Thus, our map would also be consistent with stalling on poly(A) stretches of mitochondrial mRNAs. As seen previously in cytosolic ribosomes, base-stacked poly(A) nucleotides induce A1562 but not A1561 to flip out and participate in the stack. The stack is capped at the 3’ end by C1485.

Following peptidyl transfer, the GTPase mtEF-G1 translocates the A/P and P/E hybrid tRNAs (rotated-2) into the P/P and E/E states, respectively, accompanied by a corresponding movement of the mRNA. We determined a 3.7 Å resolution structure of an mtEF-G1•GMPPCP-bound mitoribosome in the post-translocation state with P/P and E/E tRNAs and a nascent polypeptide chain (Figure 3E).

The bacterial elongation factor EF-G•GTP is bifunctional and not only translocates mRNA-tRNA through the ribosome, but also recycles the ribosome after termination, in conjunction with ribosome release factor (RRF). In human mitochondria, these roles are fulfilled by two EF-G paralogs, mtEF-G1 and mtEF-G2, respectively (29). mtEF-G1 is a homolog of bacterial EF-G with an identical five-domain architecture (30) (Figure S10D, S11E-H). The GTP binding domain I(G) is in a pre-hydrolysis conformation as previously described in

bacteria (30). Switch loops I and II are ordered around the bound GMPPCP (Figure S11G, inset).

Electron cryotomographic studies have observed human mitoribosomes at the mitochondrial inner membrane, likely in complex with the translocase Oxa1L (13). A direct connection between mitoribosomes and Oxa1L would facilitate co-translational insertion of mitochondrial proteins. To investigate nascent chain translocation, we performed focused classification with signal subtraction (FCwSS) on the ribosomal exit tunnel using particles from the whole dataset (Figure S3). Oxa1L was present in our samples as confirmed by western immunoblotting and mass spectrometry (Figure S1B, C) and is also seen in both LSU and monosome maps (Figure S3, S12A), providing evidence that normal translational elongation as well as rescue and recycling occur during nascent chain insertion into the mitochondrial inner membrane. The best map of Oxa1L was obtained from one additional round of FCwSS around the exit tunnel on the 39S particles and refined to 3.1 Å (Figure S3, S12). Most of Oxa1L was at low resolution, presumably due to inherent flexibility, and we could only model the C-terminal tail as alanines. Oxa1L contacts two mitoribosomal proteins uL24m and mL45. The C-terminal tail (30 residues) wrap over the surface of uL24m (Figure S12B). On the other side of the exit tunnel, it contacts an a-helix of mL45. The nascent chain can be traced from the 3’CCA of the P-site tRNA throughout the polypeptide tunnel and as it emerges from the tunnel exit, but becomes disordered before contacting Oxa1L.

A paradigm shift occurred in the field of translation when it was discovered that cells use the translation machinery itself to detect errors and activate quality control mechanisms. Although the existence of quality control in mitochondria was predicted based on analogy with bacteria and eukaryotic cytosols, very little was known about the molecular mechanisms. Our discovery of a mitoribosome-associated quality control pathway (Figure 4, bottom) and structural characterization of elongating mitoribosomes (Figure 4, top) now set the stage for further understanding of the regulation of mitochondrial translation. We also demonstrate that exhaustive *in silico* classification of large cryo-EM datasets can serve as a viable alternative strategy to uncover processes involved in translation in the absence of suitable *in vitro* tools.

Supplementary Material

Refer to Web version on PubMed Central for supplementary material.

Acknowledgments

We thank J. Grimmett and T. Darling for advice, data storage and high-performance computing; S. Chen, J. Brown, G. Cannone, G. Sharov for technical support; P. Emsley and G. Murshudov, P. Afonine for help with model building and refinement; S.-Y. Peak-Chew and M. Skehel for mass spectrometry analysis; T. Nakane for help with RELION; the Ramakrishnan lab members, J. L. Llácer, A. Brown and R. S. Hegde for useful discussions and reagents. We acknowledge the MRC Laboratory of Molecular Biology Electron Microscopy Facility for access and support of electron microscopy, sample preparation and data collection.

Funding

This work was supported by the UK Medical Research Council (MC_U105184332 to V.R. and MC_UU_00015/4 to M.M.), a Wellcome Trust Senior Investigator award (WT096570), the Agouron Institute, and the Louis-Jeantet

Foundation (V.R.). N.D. is funded by a Wellcome Trust Clinical PhD Fellowship (110301/Z/15/Z). H.Y. is funded by an EMBO Postdoctoral Fellowship (EMBO ALTF 806-2018).

Data and materials availability

Eight maps have been deposited into the Electron Microscopy Data Bank (EMDB) with the accession codes EMDB-11636, 11637, 11641, 11642, 11643, 11644, 11645, 11646. Six atomic coordinates have been deposited into the Proteins Data Bank under the accession codes 7A5F, 7A5G, 7A5H, 7A5I, 7A5J, 7A5K. Mass spectrometry samples report is available as a supplementary item. Further information and material requests may be made to the corresponding author.

References

1. Amunts A, Brown A, Toots J, Scheres SHW, Ramakrishnan V, Ribosome. The structure of the human mitochondrial ribosome. Science. 2015; 348:95–98. [PubMed: 25838379]
2. Desai N, Brown A, Amunts A, Ramakrishnan V. The structure of the yeast mitochondrial ribosome. Science. 2017; 355:528–531. [PubMed: 28154081]
3. Greber BJ, Bieri P, Leibundgut M, Leitner A, Aebersold R, Boehringer D, Ban N, Ribosome. The complete structure of the 55S mammalian mitochondrial ribosome. Science. 2015; 348:303–308. [PubMed: 25837512]
4. Ramrath DJF, Niemann M, Leibundgut M, Bieri P, Prange C, Horn EK, Leitner A, Boehringer D, Schneider A, Ban N. Evolutionary shift toward protein-based architecture in trypanosomal mitochondrial ribosomes. Science. 2018; 362doi: 10.1126/science.aau7735
5. Brandman O, Hegde RS. Ribosome-associated protein quality control. Nat Struct Mol Biol. 2016; 23:7–15. [PubMed: 26733220]
6. Frischmeyer PA, van Hoof A, O'Donnell K, Guerrerio AL, Parker R, Dietz HC. An mRNA surveillance mechanism that eliminates transcripts lacking termination codons. Science. 2002; 295:2258–2261. [PubMed: 11910109]
7. Ishimura R, Nagy G, Dotu I, Chuang JH, Ackerman SL. Activation of GCN2 kinase by ribosome stalling links translation elongation with translation initiation. eLife. 2016; 5:e14295. [PubMed: 27085088]
8. Balch WE, Morimoto RI, Dillin A, Kelly JW. Adapting proteostasis for disease intervention. Science. 2008; 319:916–919. [PubMed: 18276881]
9. Chiti F, Dobson CM. Protein misfolding, functional amyloid, and human disease. Annu Rev Biochem. 2006; 75:333–366. [PubMed: 16756495]
10. Ayyub SA, Gao F, Lightowlers RN, Chrzanowska-Lightowlers ZM. Rescuing stalled mammalian mitoribosomes – what can we learn from bacteria? J Cell Sci. 2020; 133:jcs231811. [PubMed: 31896602]
11. Richter R, Rorbach J, Pajak A, Smith PM, Wessels HJ, Huynen MA, Smeitink JA, Lightowlers RN, Chrzanowska-Lightowlers ZM. A functional peptidyl-tRNA hydrolase, ICT1, has been recruited into the human mitochondrial ribosome. EMBO J. 2010; 29:1116–1125. [PubMed: 20186120]
12. Pearce SF, Rorbach J, Haute LV, D'Souza AR, Rebelo-Guiomar P, Powell CA, Brierley I, Firth AE, Minczuk M. Maturation of selected human mitochondrial tRNAs requires deadenylation. eLife. 2017; 6:e27596. [PubMed: 28745585]
13. Englmeier R, Pfeffer S, Förster F. Structure of the Human Mitochondrial Ribosome Studied In Situ by Cryoelectron Tomography. Struct Lond Engl 1993. 2017; 25:1574–1581.e2.
14. Mohan S, Noller HF. Recurring RNA structural motifs underlie the mechanics of L1 stalk movement. Nat Commun. 2017; 8:1–11. [PubMed: 28232747]
15. Gopalakrishna S, Pearce SF, Dinan AM, Schober FA, Cipullo M, Spåhr H, Khawaja A, Maffezzini C, Freyer C, Wredenberg A, Atanassov I, et al. C6orf203 is an RNA-binding protein involved in mitochondrial protein synthesis. Nucleic Acids Res. 2019; 47:9386–9399. [PubMed: 31396629]

16. Chandrasekaran V, Juszkiewicz S, Choi J, Puglisi JD, Brown A, Shao S, Ramakrishnan V, Hegde RS. Mechanism of ribosome stalling during translation of a poly(A) tail. Nat Struct Mol Biol. 2019; 26:1132–1140. [PubMed: 31768042]

17. Antonicka H, Østergaard E, Sasarman F, Weraarpachai W, Wibrand F, Pedersen AMB, Rodenburg RJ, van der Knaap MS, Smeitink JAM, Chrzanowska-Lightowlers ZM, Shoubridge EA. Mutations in C12orf65 in Patients with Encephalomyopathy and a Mitochondrial Translation Defect. Am J Hum Genet. 2010; 87:115–122. [PubMed: 20598281]

18. Soleimanpour-Lichaei HR, Kühl I, Gaisne M, Passos JF, Wydro M, Rorbach J, Temperley R, Bonnefoy N, Tate W, Lightowlers R, Chrzanowska-Lightowlers Z. mtRF1a Is a Human Mitochondrial Translation Release Factor Decoding the Major Termination Codons UAA and UAG. Mol Cell. 2007; 27:745–757. [PubMed: 17803939]

19. Shimazaki H, Takiyama Y, Ishiura H, Sakai C, Matsushima Y, Hatakeyama H, Honda J, Sakoe K, Naoi T, Namekawa M, Fukuda Y, et al. Japan Spastic Paraplegia Research Consortium (JASPAC), A homozygous mutation of C12orf65 causes spastic paraplegia with optic atrophy and neuropathy (SPG55). J Med Genet. 2012; 49:777–784. [PubMed: 23188110]

20. Wesolowska M, Gorman GS, Alston CL, Pajak A, Pyle A, He L, Griffin H, Chinnery PF, Miller JAL, Schaefer AM, Taylor RW, et al. Adult Onset Leigh Syndrome in the Intensive Care Setting: A Novel Presentation of a C12orf65 Related Mitochondrial Disease. J Neuromuscul Dis. 2015; 2:409–419. [PubMed: 27858754]

21. Su T, Izawa T, Thoms M, Yamashita Y, Cheng J, Berninghausen O, Hartl FU, Inada T, Neupert W, Beckmann R. Structure and function of Vms1 and Arb1 in RQC and mitochondrial proteome homeostasis. Nature. 2019; 570:538–542. [PubMed: 31189955]

22. Yip MCJ, Keszei AFA, Feng Q, Chu V, McKenna MJ, Shao S. Mechanism for recycling tRNAs on stalled ribosomes. Nat Struct Mol Biol. 2019; 26:343–349. [PubMed: 31011209]

23. Brown A, Rathore S, Kimanius D, Aibara S, Bai X, Rorbach J, Amunts A, Ramakrishnan V. Structures of the human mitochondrial ribosome in native states of assembly. Nat Struct Mol Biol. 2017; 24:866–869. [PubMed: 28892042]

24. Gartmann M, Blau M, Armache J-P, Mielke T, Topf M, Beckmann R. Mechanism of eIF6-mediated inhibition of ribosomal subunit joining. J Biol Chem. 2010; 285:14848–14851. [PubMed: 20356839]

25. Heuer A, Gerovac M, Schmidt C, Trowitzsch S, Preis A, Kötter P, Berninghausen O, Becker T, Beckmann R, Tampé R. Structure of the 40S–ABCE1 post-splitting complex in ribosome recycling and translation initiation. Nat Struct Mol Biol. 2017; 24:453–460. [PubMed: 28368393]

26. Kolupaeva VG, Unbehaun A, Lomakin IB, Hellen CUT, Pestova TV. Binding of eukaryotic initiation factor 3 to ribosomal 40S subunits and its role in ribosomal dissociation and anti-association. RNA N Y N. 2005; 11:470–486.

27. Mancera-Martínez E, Brito Querido J, Valasek LS, Simonetti A, Hashem Y. ABCE1: A special factor that orchestrates translation at the crossroad between recycling and initiation. RNA Biol. 2017; 14:1279–1285. [PubMed: 28498001]

28. Voorhees RM, Schmeing TM, Kelley AC, Ramakrishnan V. The mechanism for activation of GTP hydrolysis on the ribosome. Science. 2010; 330:835–838. [PubMed: 21051640]

29. Mai N, Chrzanowska-Lightowlers ZMA, Lightowlers RN. The process of mammalian mitochondrial protein synthesis. Cell Tissue Res. 2017; 367:5–20. [PubMed: 27411691]

30. Gao Y-G, Selmer M, Dunham CM, Weixlbaumer A, Kelley AC, Ramakrishnan V. The structure of the ribosome with elongation factor G trapped in the posttranslocational state. Science. 2009; 326:694–699. [PubMed: 19833919]

31. Zivanov J, Nakane T, Forsberg BO, Kimanius D, Hagen WJ, Lindahl E, Scheres SH. New tools for automated high-resolution cryo-EM structure determination in RELION-3. eLife. 2018; 7:e42166. [PubMed: 30412051]

32. Rosenthal PB, Henderson R. Optimal Determination of Particle Orientation, Absolute Hand, and Contrast Loss in Single-particle Electron Cryomicroscopy. J Mol Biol. 2003; 333:721–745. [PubMed: 14568533]

33. Zheng SQ, Palovcak E, Armache J-P, Verba KA, Cheng Y, Agard DA. MotionCor2: anisotropic correction of beam-induced motion for improved cryo-electron microscopy. Nat Methods. 2017; 14:331–332. [PubMed: 28250466]
34. Rohou A, Grigorieff N. CTFFIND4: Fast and accurate defocus estimation from electron micrographs. J Struct Biol. 2015; 192:216–221. [PubMed: 26278980]
35. Casañal A, Lohkamp B, Emsley P. Current developments in Coot for macromolecular model building of Electron Cryo-microscopy and Crystallographic Data. Protein Sci Publ Protein Soc. 2020; 29:1069–1078.
36. Afonine PV, Poon BK, Read RJ, Sobolev OV, Terwilliger TC, Urzhumtsev A, Adams PD. Real-space refinement in PHENIX for cryo-EM and crystallography. Acta Crystallogr Sect Struct Biol. 2018; 74:531–544.
37. Liebschner D, Afonine PV, Baker ML, Bunkóczi G, Chen VB, Croll TI, Hintze B, Hung LW, Jain S, McCoy AJ, Moriarty NW, et al. Macromolecular structure determination using X-rays, neutrons and electrons: recent developments in Phenix. Acta Crystallogr Sect Struct Biol. 2019; 75:861–877.
38. Andersen GR, Thirup S, Spremulli LL, Nyborg J. High resolution crystal structure of bovine mitochondrial EF-tu in complex with GDP11. Nagai K. J Mol Biol. 2000; 297:421–436. [PubMed: 10715211]
39. Yang J, Zhang Y. I-TASSER server: new development for protein structure and function predictions. Nucleic Acids Res. 2015; 43:W174–181. [PubMed: 25883148]
40. Waterhouse A, Bertoni M, Bienert S, Studer G, Tauriello G, Gumienny R, Heer FT, de Beer TAP, Rempfer C, Bordoli L, Lepore R, et al. SWISS-MODEL: homology modelling of protein structures and complexes. Nucleic Acids Res. 2018; 46:W296–W303. [PubMed: 29788355]
41. Biesiada, M, Purzycka, KJ, Szachniuk, M, Blazewicz, J, Adamiak, RW. RNA Structure Determination: Methods and ProtocolsMethods in Molecular Biology. Turner, DH, Mathews, DH, editors. Springer; New York, NY: 2016. 199–215.
42. Lorenz R, Bernhart SH, Höner Zu Siederdissen C, Tafer H, Flamm C, Stadler PF, Hofacker IL. ViennaRNA Package 2.0. Algorithms Mol Biol AMB. 2011; 6:26. [PubMed: 22115189]
43. Nicholls RA, Long F, Murshudov GN. Low-resolution refinement tools in REFMAC5. Acta Crystallogr D Biol Crystallogr. 2012; 68:404–417. [PubMed: 22505260]
44. Rae CD, Gordiyenko Y, Ramakrishnan V. How a circularized tmRNA moves through the ribosome. Science. 2019; 363:740–744. [PubMed: 30765567]
45. Endo, Y, Takai, K, Ueda, T. Cell-Free Protein ProductionMethods in Molecular Biology. Vol. 607. Humana Press; Totowa, NJ: 2010.
46. Perkins DN, Pappin DJ, Creasy DM, Cottrell JS. Probability-based protein identification by searching sequence databases using mass spectrometry data. Electrophoresis. 1999; 20:3551–3567. [PubMed: 10612281]
47. Keller A, Nesvizhskii AI, Kolker E, Aebersold R. Empirical statistical model to estimate the accuracy of peptide identifications made by MS/MS and database search. Anal Chem. 2002; 74:5383–5392. [PubMed: 12403597]
48. Pettersen EF, Goddard TD, Huang CC, Couch GS, Greenblatt DM, Meng EC, Ferrin TE. UCSF Chimera--a visualization system for exploratory research and analysis. J Comput Chem. 2004; 25:1605–1612. [PubMed: 15264254]
49. Fang X-J, Zhang W, Lyu H, Wang Z-X, Wang W-W, Yuan Y. Compound Heterozygote Mutation of C12orf65 Causes Distal Motor Neuropathy and Optic Atrophy. Chin Med J (Engl). 2017; 130:242–244. [PubMed: 28091420]
50. Imagawa E, Fattal-Valevski A, Eyal O, Miyatake S, Saada A, Nakashima M, Tsurusaki Y, Saitsu H, Miyake N, Matsumoto N. Homozygous p.V116* mutation in C12orf65 results in Leigh syndrome. J Neurol Neurosurg Psychiatry. 2016; 87:212–216. [PubMed: 25995486]
51. Nishihara H, Omoto M, Takao M, Higuchi Y, Koga M, Kawai M, Kawano H, Ikeda E, Takashima H, Kanda T. Autopsy case of the C12orf65 mutation in a patient with signs of mitochondrial dysfunction. Neurol Genet. 2017; 3doi: 10.1212/NXG.0000000000000171

52. Heidary G, Calderwood L, Cox GF, Robson CD, Teot LA, Mullon J, Anselm I. Optic atrophy and a Leigh-like syndrome due to mutations in the c12orf65 gene: report of a novel mutation and review of the literature. J Neuro-Ophthalmol Off J North Am Neuro-Ophthalmol Soc. 2014; 34:39–43.

53. Spiegel R, Mandel H, Saada A, Lerer I, Burger A, Shaag A, Shalev SA, Jabaly-Habib H, Goldsher D, Gomori JM, Lossos A, et al. Delineation of C12orf65-related phenotypes: a genotype-phenotype relationship. Eur J Hum Genet EJHG. 2014; 22:1019–1025. [PubMed: 24424123]

54. Buchert R, Uebe S, Radwan F, Tawamie H, Issa S, Shimazaki H, Henneke M, Ekici AB, Reis A, Abou Jamra R. Mutations in the mitochondrial gene C12ORF65 lead to syndromic autosomal recessive intellectual disability and show genotype phenotype correlation. Eur J Med Genet. 2013; 56:599–602. [PubMed: 24080142]

55. Tucci A, Liu Y-T, Preza E, Pitceathly RDS, Chalasani A, Plagnol V, Land JM, Trabzuni D, Ryten M, UKBEC, Jaunmuktane Z, et al. Novel C12orf65 mutations in patients with axonal neuropathy and optic atrophy. J Neurol Neurosurg Psychiatry. 2014; 85:486–492. [PubMed: 24198383]

Europe PMC Funders Author Manuscripts

Europe PMC Funders Author Manuscripts

Once sentence summary

Elongationally-stalled mitochondrial ribosomes are rescued by a mitoribosome-associated quality control pathway.

Europe PMC Funders Author Manuscripts

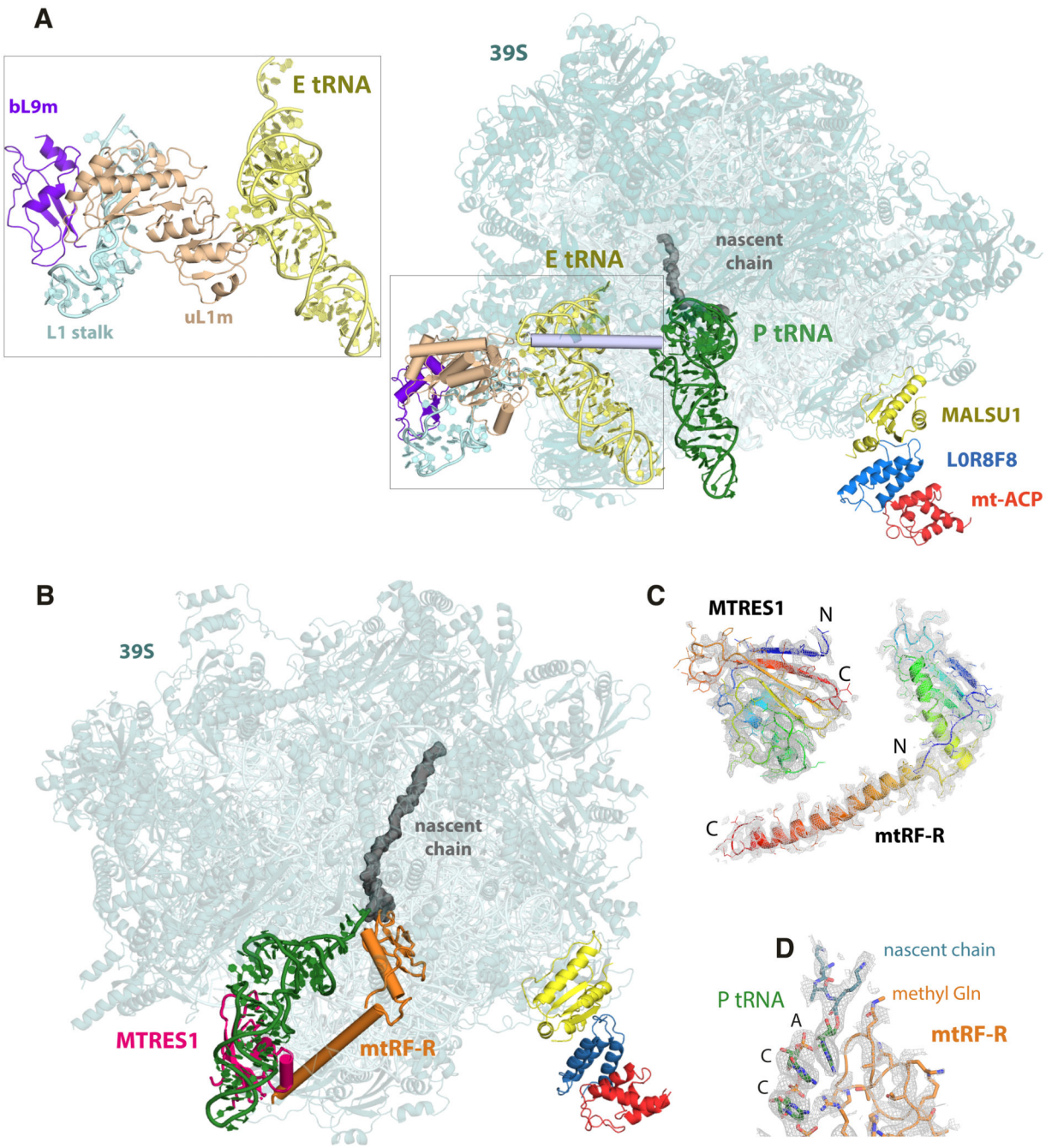

Fig. 1. Structures of split mitoribosome intermediates undergoing quality control

A) Overall structure of mitochondrial large subunit complexed with P, E tRNAs, nascent chain and elements of proteins of the large subunit. (inset) Packing interactons between the D-loop of the E-site tRNA and the L1 stalk. (B) Overall structure of mitochondrial large subunit in complex with a P tRNA, nascent chain, mtRF-R and MTRES1. (C) Map-model fits for MTRES1 (lef) and mtRF-R (right). The N- (blue) and C- (red) terminal ends are indicated. The good local resoluton permits unambiguous assignment of the backbone and most sidechains (shown as lines). (D) Close up view of the ribosomal peptdyl trans-ferase

center (PTC) showing cryo-EM density for interactons between the CCA end of the P tRNA and the GGQ domain of mtRF-R poised to hydrolyse the nascent chain.

Europe PMC Funders Author Manuscripts

Europe PMC Funders Author Manuscripts

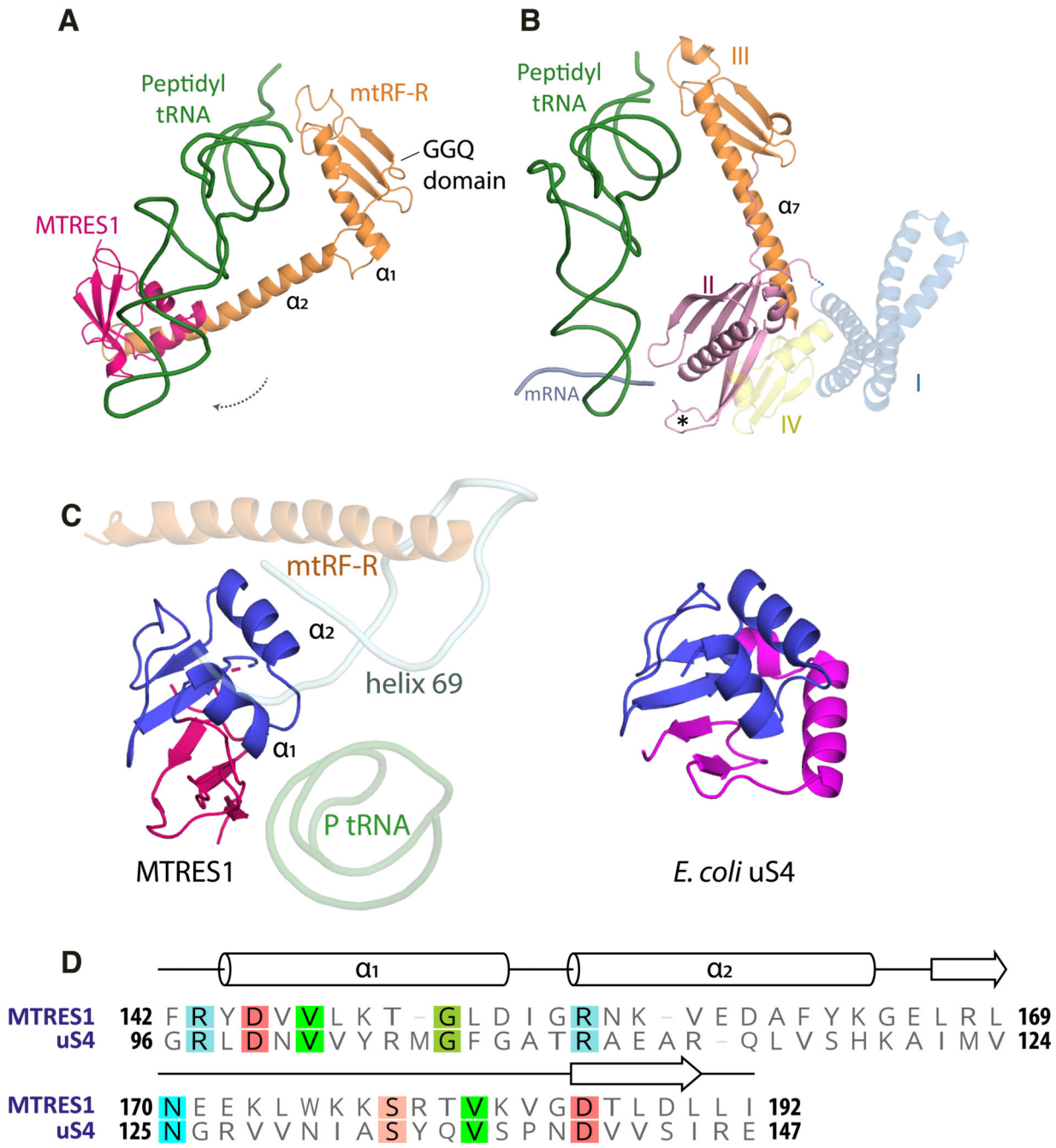

Fig. 2. Comparison of mtRF-R and MTRES1 with bacterial homologues

A) mtRF-R (orange) and MTRES1 (dark pink) together resemble domains II and III in bacterial RF2. The peptdyl tRNA has been repositoned towards the E site (doted arrow) and the long α2-helix of domain III has remodeled to bind MTRES1, which wraps around the peptdyl tRNA. (B) Bacterial class I release factor (domain I, blue; domain II, pink; domain III, orange; domain IV, yellow) in the A site of a terminatng 70S ribosome. The peptdyl tRNA (green) and mRNA (blue grey) are also shown. The asterisk indicates the PXT motf that recognizes the stop codon (PDB 5MDV). (C) Comparison of *E. coli* uS4 and human

MTRES1. The structurally conserved dsRNA-binding region is shown in blue. Note that the rest of the proteins are topologically different (magenta vs dark pink). (D) Structure-based alignment and secondary structure of the two proteins.

Europe PMC Funders Author Manuscripts

Europe PMC Funders Author Manuscripts

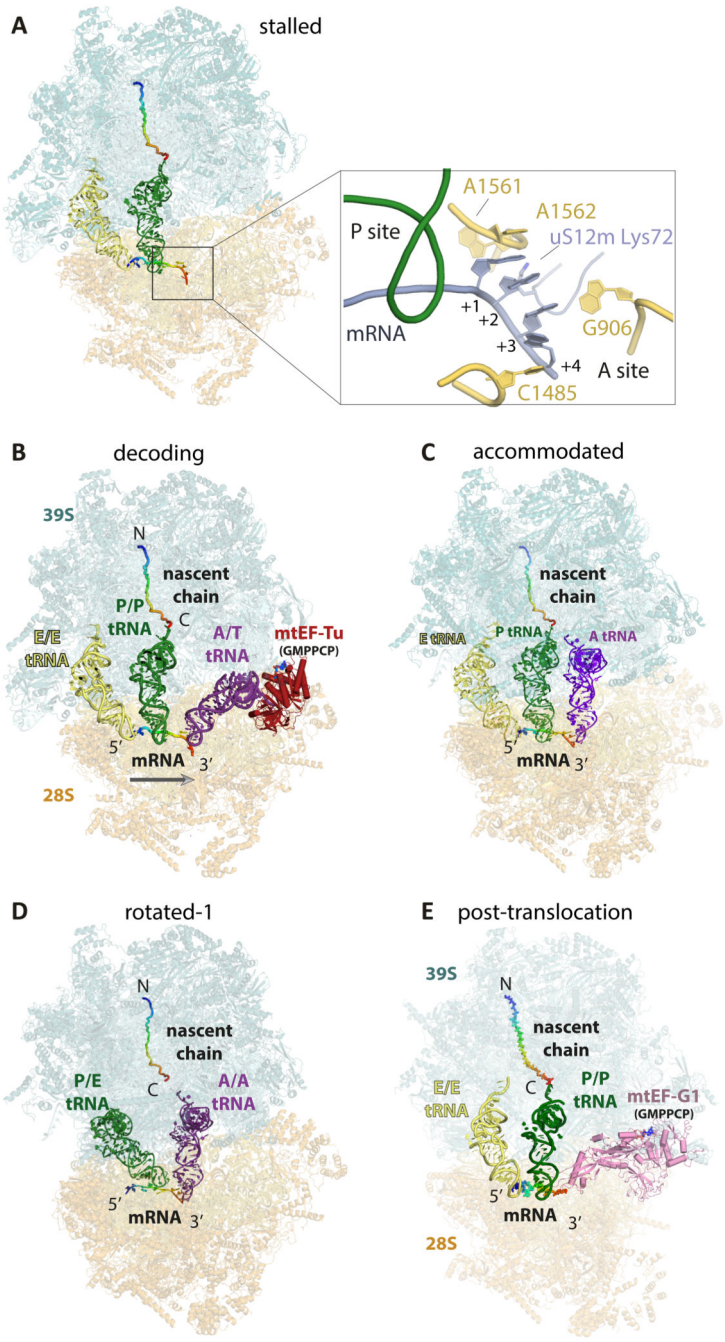

Fig. 3. Structures of active and stalled elongation intermediates

(A) Structure of an elongatng mitoribosome stalled with an empty A site and bound to P- (green) and E-site (yellow) tRNAs. (Inset) Close-up view of interactons between the mRNA (pale blue) and decoding bases of the 12S rRNA (yellow). (B) Elongatng mitori-bosome-nascent chain complex during decoding of an incoming A/T tRNA bound to mitochondrial elongaton factor Tu (mtEF-Tu). The arrow indicates the directon of translaton. (C) Canonical state bound to A, P and E tRNAs. (D) Rotated-1 state with A/A and P/E tRNAs. The nascent chain is atached to the A/A tRNA but the ester bond is not seen due to poor resoluton.

Coordinates not deposited. (E) Post-translocated state bound to mitochondrial elongaton factor G1.

Europe PMC Funders Author Manuscripts

Europe PMC Funders Author Manuscripts

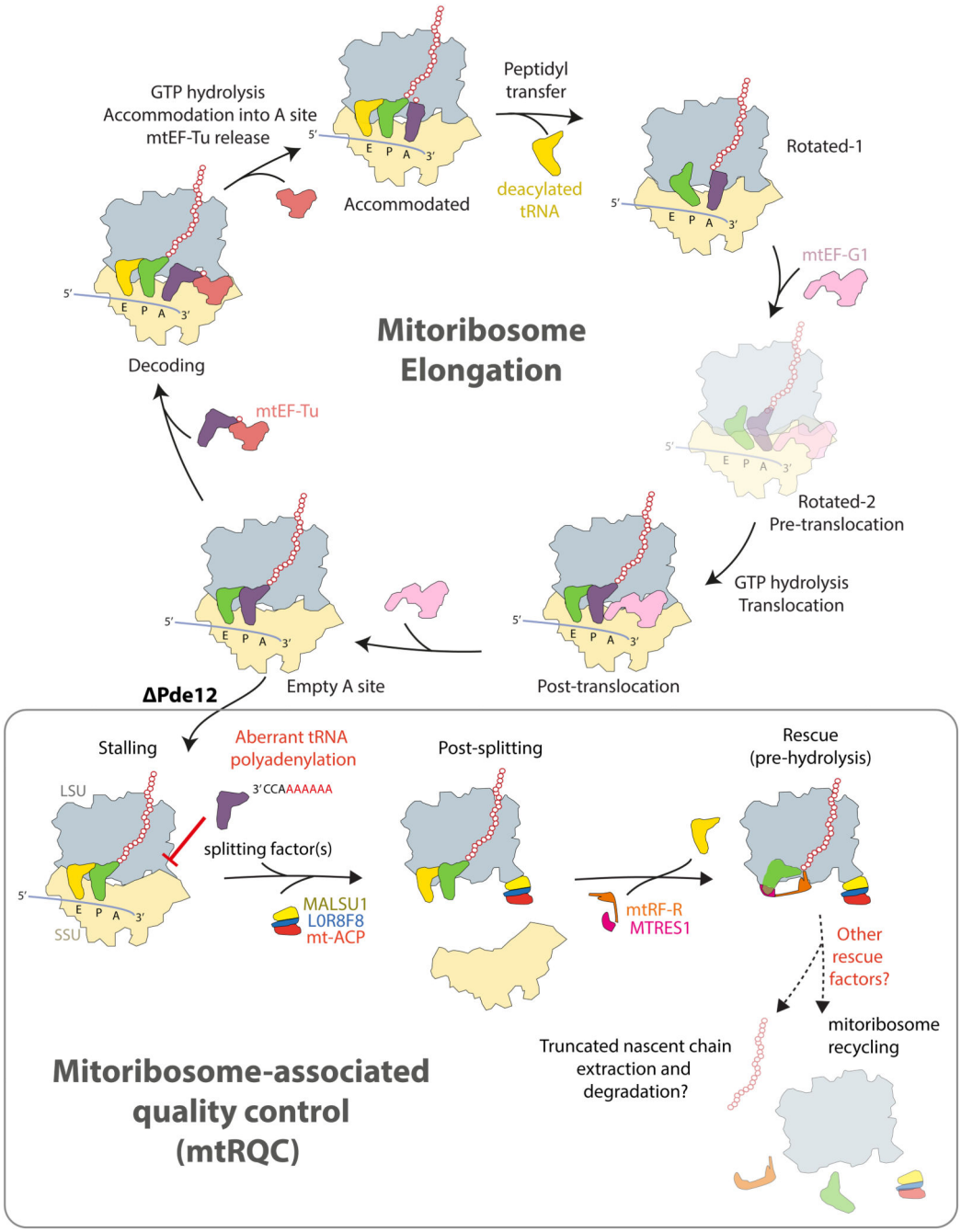

Fig. 4. Schematic of the mitoribosomal elongation cycle (top) and mitoribosome associated quality control (bottom)

States visualized in this study are opaque. States not visualized in this study are translucent. PDB codes of bacterial counterparts to these states are 4V5F (post-translocaton), 6WD0 (empty A-site), 4V5L (decoding), 6WDD (accommodated).